

A pulse radiolysis study of free radicals formed by one-electron oxidation of the antimalarial drug pyronaridine

Fyaz M. D. Ismail · Michael G. B. Drew ·
Suppiah Navaratnam · Roger H. Bisby

Received: 30 October 2008 / Accepted: 5 December 2008 / Published online: 9 June 2009
© Springer Science+Business Media BV 2009

Abstract Free radicals from one-electron oxidation of the antimalarial drug pyronaridine have been studied by pulse radiolysis. The results show that pyronaridine is readily oxidised to an intermediate semi-iminoquinone radical by inorganic and organic free radicals, including those derived from tryptophan and acetaminophen. The pyronaridine radical is rapidly reduced by both ascorbate and caffeic acid. The results indicate that the one-electron reduction potential of the pyronaridine radical at neutral pH lies between those of acetaminophen (707 mV) and caffeic acid (534 mV). The pyronaridine radical decays to produce the iminoquinone, detected by electrospray mass spectrometry, in a second-order process that density functional theory (DFT) calculations (UB3LYP/6-31+G*) suggest is a disproportionation reaction. Important calculated dimensions of pyronaridine, its phenoxyl and aminyl radical, as well as the iminoquinone, are presented.

Keywords Pyronaridine · Free radical · Pulse radiolysis · Oxidation · DFT · Antimalarial

Electronic supplementary material The online version of this article (doi:10.1007/s11164-009-0051-7) contains supplementary material, which is available to authorized users.

F. M. D. Ismail
School of Pharmacy and Biomolecular Sciences, Liverpool John Moores University,
Liverpool L3 3AF, UK

M. G. B. Drew
Department of Chemistry, University of Reading, Reading RG6 6AD, UK

S. Navaratnam · R. H. Bisby (✉)
Biomedical Sciences Research Institute, University of Salford, Salford M5 4WT, UK
e-mail: r.h.bisby@salford.ac.uk

S. Navaratnam
Free Radical Research Facility, STFC Daresbury Laboratory, Warrington WA4 4AD, UK

Introduction

The massive problem of endemic and drug-resistant malaria in tropical countries, especially that due to potentially fatal infections with *Plasmodium falciparum*, has led to the development of a wide range of antimalarial drugs [1]. Pyronaridine (Fig. 1) was introduced as an antimalarial agent in the 1970s as a development of the existing antimalarial drug amodiaquine [2, 3]. Although an effective antimalarial agent, amodiaquine has the potential to induce potentially fatal hepatotoxicity [4] and has now been withdrawn from use, except in the treatment of acute and resistant infections. The toxicity of amodiaquine results from oxidation of the aminophenol function, probably through the intermediate formation of the semi-iminoquinone radical [5], and the formation of a reactive iminoquinone [6–9]. In comparison, pyronaridine shows less clinical toxicity but retains some of the biochemical properties associated with amodiaquine toxicity, such as oxidation by peroxidases, iminoquinone formation, glutathione depletion and cytotoxicity [6]. These reactions of the aminophenol function in antimalarial drugs reflect the well known toxicity of the same group within acetaminophen (*N*-acetylaminophenol, APAP) [10]. The pyronaridine molecule is normally formulated for clinical use as the tetraphosphate and Fig. 1 indicates the pK_a values for proton loss at the various sites in the molecule [11]. Pyronaridine is of particular interest since it has been reported to be active against multidrug-resistant strains of *Plasmodium* [12], inhibits *Plasmodium falciparum* topoisomerase II [13] and is being evaluated for worldwide prophylactic use against all strains (drug-resistant and -sensitive) of malaria [1].

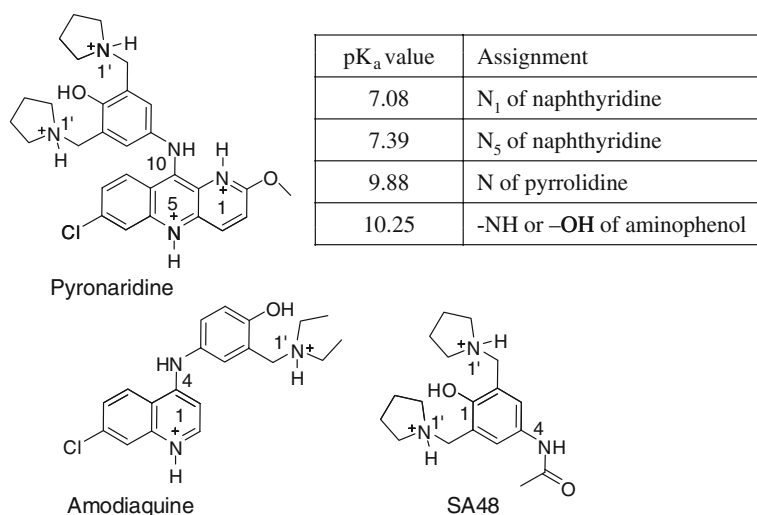


Fig. 1 Structures of the antimalarial drugs pyronaridine (malaridine; Drug 7351 or 4-[(7-chloro-2-methoxybenzo[b]-1,5-naphthyridin-10-yl)amino]-2,6-bis(1-pyrrolidinylmethyl)-phenol) and amodiaquine (4-(7-chloroquinolin-4-ylamino)-2-((diethylamino)methyl)phenol), together with that of the model compound SA48 (*N*-(4-hydroxy-3,5-bis(pyrrolidin-1-ylmethyl)phenyl)acetamide). The table indicates the pK_a values and sites of ionisation in the pyronaridine molecule (from reference [11])

The propensity for oxidation of the aminophenol function in both amodiaquine and pyronaridine is involved not only in toxic side effects, but may also be involved in their modes of antimalarial action. In the intra-erythrocytic stage, the malaria parasite degrades haemoglobin and utilises the released amino acids for its own catabolism [14]. The haeme that is simultaneously released is potentially toxic to the parasite through reactions that induce oxidative stress and contribute to the pathophysiology of fatal cerebral malaria [15]. Biocrystallisation of the free haeme, which may be a spontaneous or enzymically promoted process [16], produces redox inactive β -haematin, also known as haemozoin or malaria pigment [17]. This eliminates oxidative stress due to free haeme and allows the parasite to survive. Compounds that inhibit haeme biocrystallisation may also possess antimalarial activity [18]. Recent results indicate that pyronaridine forms a complex with haematin that inhibits further biocrystallisation [19]. This is now considered to be the mode of action rather than inhibition of parasite topoisomerase [13]. Such interactions appear to depend on a slipped offset interaction [3, 18] rather than the previously assumed π - π interactions between drug and haematin, with the drug acting as a partial electron donor.

Pulse radiolysis studies have previously been used to study the redox behaviour of phenols and aminophenols and the properties of the phenoxyl and semi(imino)quinone radicals formed by one-electron oxidation [20, 21]. Pulse radiolysis studies of both APAP [22] and amodiaquine [23] have been reported. The present pulse radiolysis study has been undertaken to assess the reactivity and reduction potential of the intermediate free radical formed by one-electron oxidation of pyronaridine.

Materials and methods

Pyronaridine tetraphosphate was a gift from Professor D. Warhurst (London School of Hygiene and Tropical Medicine). The model compound *N*-(4-hydroxy-3,5-bis(pyrrolidin-1-ylmethyl)phenyl)acetamide, SA48, was prepared by a published procedure [24]. Other chemicals used were of Analar grade and solutions were prepared in water obtained from a Millipore Milli-Q unit or equivalent.

Pulse radiolysis was undertaken using the Daresbury linear accelerator with pulses of 12-MeV electrons [25]. The radiation dose was between approximately 2 and 12 Gy per pulse, with a pulse length of 200 ns. The solution was irradiated in a quartz capillary cell with an optical path length of 2.5 cm and dosimetry was performed with an air-saturated solution of KSCN (10 mmol dm⁻³).

The oxidation products of pyronaridine pulse radiolysis were studied using positive-ion electrospray mass spectroscopy (PI-ESMS) in LockSpray mode [18]. The irradiated solution was evaporated to dryness and re-dissolved in ethyl acetate (10 mL). The upper organic layer was exhaustively vortexed with HPLC-grade water to remove azide and other inorganic materials (washed \times 10 times; total volume 25 mL). An approximately 10×10^{-6} mol dm⁻³ solution of the organic components was prepared in methanol and infused at a rate of 10 μ L min⁻¹ into the mass spectrometer (LCT-TOF MS, Micromass Limited, Manchester, U.K.). The spectrometer was operated using factory-standard settings modified as follows:

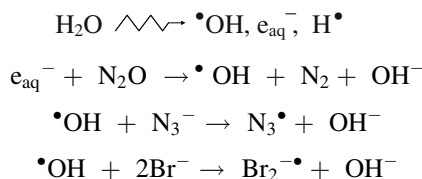
extraction cone = 3 V; sample cone = 30 V, RF lens = 250 V; ionisation potential 3,000 V; pusher time = 60 ms; desolvation temperature = 150°C; source temperature = 100°C. Under these conditions, pyronaridine ($C_{29}H_{33}ClN_5O_2+$; Exact Mass: 518.23173) formed only a small amount of the corresponding iminoquinone ($C_{29}H_{31}ClN_5O_2+$; Exact Mass: 516.21608) Compound identities of irradiated products were verified by comparison with data obtained involving authentic pyronaridine and pyronaridine iminoquinone.

Synthesis of 7-chloro-2-methoxybenzo[*b*][1,5]naphthyridin-10-ylimino)-2,6-bis(pyrrolidin-1-ylmethyl)cyclohexa-2,5-dienone: pyronaridine tetraphosphate 0.0934 g (1.03×10^{-4} moles; $C_{29}H_{44}ClN_5O_{18}P_4$; RMM = 910.03) was intimately mixed with solid potassium ferricyanide (0.1171 g, 3.56×10^{-4} moles) to which 4 mL of 0.1 M, ice cold NaOH, was added and vigorously vortexed for one minute. A small exotherm was evident, with rapid darkening of the reactants to provide a deep beetroot-coloured suspension. Two millilitres of hexane was added and the vessel sealed with a cap. The sample was incubated with stirring at 40°C using focused microwave irradiation (CEM Corporation, 5 W) for 15 min. The sample was left to stand for 12 h at 25°C in absolute darkness. Working under subdued lighting conditions, the upper purple-tinged hexane layer was aspirated and washed with water (3×5 mL), dried with anhydrous magnesium sulphate and then evaporated to dryness under a stream of dry nitrogen. The material was re-suspended in MeOH (2 mL) and evaporated to yield the magenta-coloured iminoquinone (0.0522 g, 1.02×10^{-4} moles, 99%; $C_{29}H_{30}ClN_5O_2$; RMM = 515.21), which possessed a bronze lustre. The compound was characterised by high-resolution PI-ESMS ($C_{29}H_{30}ClN_5O_2^+$ Expected Exact Mass: 516.21608, Found = 516.2161).

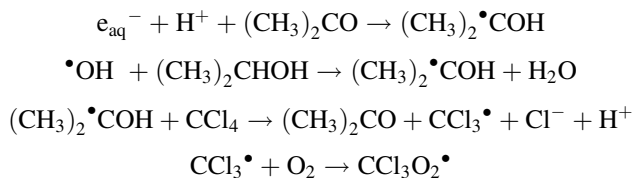
Results

Oxidation of pyronaridine by inorganic radicals

The oxidising inorganic radicals N_3^\bullet (E_o' 1.33 V [26]) and $Br_2^{\bullet-}$ (E_o' 1.66 V [26]) were produced by pulse radiolysis of N_2O -saturated solutions containing the corresponding salt:



In addition, the oxidising trichloromethylperoxyl radical, $CCl_3O_2^\bullet$ (E_o' 1.3 V [26]), was produced in solutions saturated with N_2O/O_2 (4:1 v/v) containing acetone, propan-2-ol and CCl_4 :



At $\text{pH} < 7$, both azidyl radical and dibromide radical anion reacted with pyronaridine to produce a product radical with absorption maxima in the measured difference spectrum at 540 and 630 nm (Fig. 2a, b). The difference spectra also displayed bleaching in the region of the long-wavelength absorption maximum of pyronaridine at 430 nm (Fig. 2b). As the pH was increased, the transient absorption spectrum resulting from oxidation by azidyl radicals (Fig. 2a) was transformed to one with absorption maxima at 490 and 600 nm, with isobestic points at ca. 555 and 630 nm. The transient spectra obtained by the oxidation of pyronaridine by the trichloromethylperoxyl radical at pH 7.7 (Fig. 2b) was very similar to that formed by the reaction of azidyl radical at the same pH value. The similarity in transient absorption spectra at a particular pH value produced by the different oxidising free radicals indicates that reaction occurs by simple one-electron oxidation and that the shift in the spectrum with pH results from deprotonation of the radical.

For comparison, the transient absorption spectra obtained by one-electron oxidation of the model compound 4-amino-2,6-*bis*(1-pyrrolidinylmethyl)-phenol (SA48, Fig. 1) are shown in Fig. 3. The transient spectra show maxima at 450 nm at pH 6.8 and 500 nm at pH 12.8, which are very similar to those observed previously for APAP [22], with the change resulting from deprotonation of the phenoxyl radical at the nitrogen atom with a pK_a of 11.1. Second-order rate constants for the reaction of oxidising free radicals with pyronaridine and related compounds are shown in Table 1. Azidyl radicals were found to react with pyronaridine, amodiaquine, APAP and SA48 at neutral pH, with rate constants in excess of $10^9 \text{ dm}^3 \text{ mol}^{-1} \text{ s}^{-1}$, close to the diffusion-controlled limit and consistent with the high reduction potential for $\text{N}_3\bullet$. In alkaline solution, the rate constants all increase due to deprotonation of the phenolic group (pK_a ca 10). However, measurements with pyronaridine were limited by it being virtually insoluble at $\text{pH} > 10$. Deprotonation of the pyrrolidine groups in pyronaridine and SA28 appear to have little effect on the rate of oxidation by the azidyl radical. At neutral pH, the second-order rate constant for the reaction of dibromide radical anion decreases by two orders of magnitude in the order pyronaridine > amodiaquine > APAP, and is taken to reflect both the influence of the positively charged pyrrolidine groups and the lower reduction potentials for amodiaquine and pyronaridine compared with APAP (see below). The electrophilic trichloromethylperoxyl radical ($\text{CCl}_3\text{O}_2\bullet$) was also found to oxidise pyronaridine very rapidly, with a second-order rate constant of $1.8 \times 10^9 \text{ dm}^3 \text{ mol}^{-1} \text{ s}^{-1}$. These results suggest that the aminophenol moiety of pyronaridine is the principle site for reaction with oxidising free radicals.

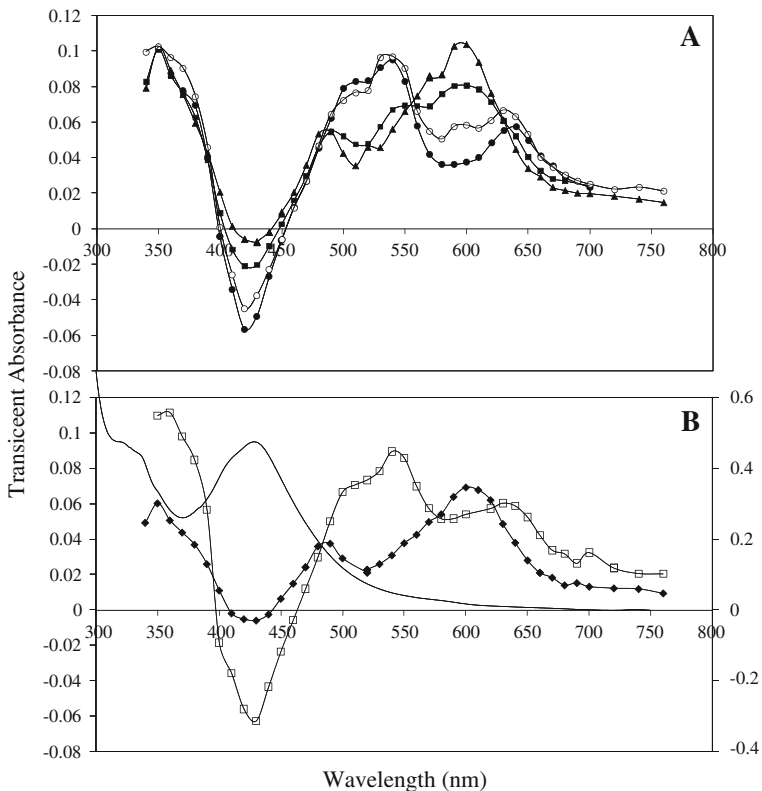
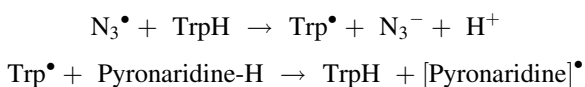


Fig. 2 **a** Transient spectra formed by the oxidation of pyronaridine by azidyl radical in N_2O -saturated solutions containing pyronaridine ($50 \mu\text{mol dm}^{-3}$) and sodium azide (0.1 mol dm^{-3}) at pH 5.4 40 μs after the pulse (filled circle), pH 6.7 40 μs after the pulse (open circle), pH 7.6 20 μs after the pulse (filled square) and pH 8.8 20 μs after the pulse (filled triangle). **b** Transient spectra from the oxidation of pyronaridine ($50 \mu\text{mol dm}^{-3}$) by $\text{Br}_2^{\bullet-}$ in N_2O -saturated solution containing KBr (0.1 mol dm^{-3}) at pH 6.8 40 μs after the pulse (open square) and by trichloromethylperoxyl radical at pH 7.7 50 μs after the pulse (filled diamond) in a solution saturated with N_2O/O_2 (4:1 v/v) and containing propan-2-ol (3.3 mol dm^{-3}), acetone (1.4 mol dm^{-3}) and carbon tetrachloride (12 mmol dm^{-3}). Dose = 9 Gy per pulse. The absorption spectrum of unirradiated pyronaridine ($50 \mu\text{mol dm}^{-3}$) at pH 8.8 is shown for comparison (solid lines)

Free radical interactions between pyronaridine and organic compounds

In aqueous solution at neutral pH, tryptophan was oxidised to the neutral indolyl radical (λ_{max} 520 nm) by azidyl radicals. The indolyl radical from tryptophan is relatively oxidising (E_o' 1.015 V [27]) and in the presence of pyronaridine was found to react, as shown by the formation of the characteristic 640-nm absorption of the pyronaridine radical at neutral pH, as illustrated in Fig. 4:



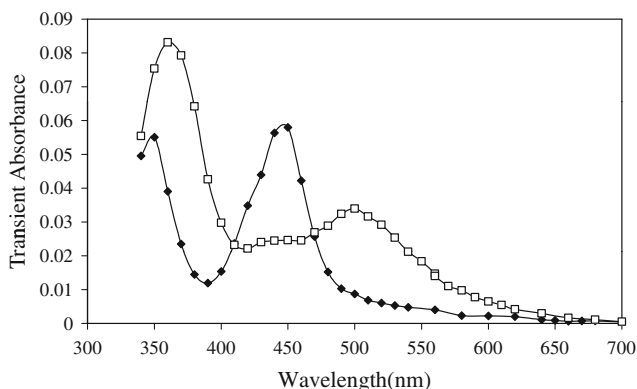


Fig. 3 Transient absorption spectra from one-electron oxidation of SA48 by azidyl radicals at pH 6.8 (filled diamond) and at pH 12.8 (open square)

Table 1 Second-order rate constants (units, $\text{dm}^3 \text{mol}^{-1} \text{s}^{-1}$) for reaction at neutral pH (unless otherwise indicated) of some inorganic radicals with pyronaridine and related compounds

Radical species	Pyronaridine	Amodiaquine ^a	APAP ^b	SA48
N_3^\bullet	3.5×10^9 (pH 6.8) 5.2×10^9 (pH 9.2)	1.2×10^9	3.8×10^9 (pH 7.1) 5.8×10^9 (pH 11.1)	2.4×10^9 (pH 6.8) 3.2×10^9 (pH 12.8)
$\text{Br}_2^{\bullet-}$	3.0×10^9 (pH 6.8)	2.1×10^8	2.5×10^7	–
$\text{CCl}_3\text{O}_2^\bullet$	1.8×10^9 (pH 7.7)	–	–	–

^a From reference [23]

^b From reference [22]

The second-order rate constant for the oxidation of pyronaridine by tryptophanyl radicals was found to be $(8.0 \pm 0.4) \times 10^7 \text{ dm}^3 \text{mol}^{-1} \text{ s}^{-1}$ from the second-order plot in the inset of Fig. 4. The lower rate constant by over an order of magnitude compared with that determined with the inorganic radicals described above is due to the comparatively lower reduction potential of the tryptophanyl radical. The semi-iminoquinone free radical from APAP ($E_o' 707 \text{ mV}$ [22]) was also found to oxidise pyronaridine to the free radical with an apparent second-order rate constant of $\sim 10^8 \text{ dm}^3 \text{mol}^{-1} \text{ s}^{-1}$, as illustrated in Fig. 5.

Ascorbate is highly reducing with $E_o' (\text{Asc}^{\bullet-}, \text{H}^+/\text{AscH}^-) 300 \text{ mV}$ [20]. Accordingly, in solutions containing pyronaridine and lower concentrations of ascorbate, the absorption at 640 nm of the pyronaridine radical formed by oxidation with azidyl radical at neutral pH was found to decay exponentially with first-order rates, increasing with ascorbate concentration, as illustrated in Fig. 6. The inset of Fig. 6 shows the second-order plot giving a second-order rate constant of $(1.4 \pm 0.1) \times 10^7 \text{ dm}^3 \text{mol}^{-1} \text{ s}^{-1}$. Caffeic acid ($E_o' 534 \text{ mV}$ [28]) was similarly found to reduce the pyronaridine radical with a second-order rate constant of $(5.6 \pm 0.4) \times 10^6 \text{ dm}^3 \text{mol}^{-1} \text{ s}^{-1}$.

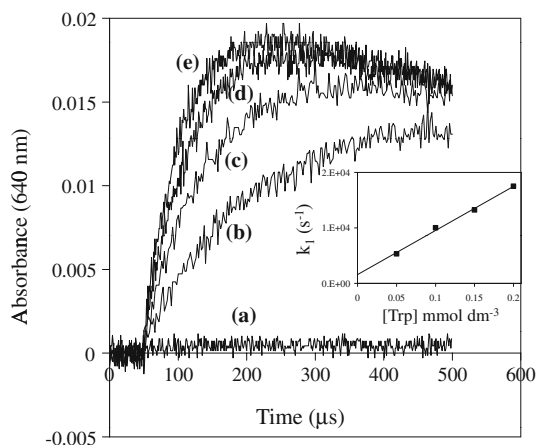


Fig. 4 Oxidation pyronaridine by tryptophan radicals demonstrated by the formation of the pyronaridine radical transient absorption at 640 nm in N_2O -saturated solutions at pH 7 containing NaN_3 (0.1 mol dm^{-3}) and tryptophan (2.5 mmol dm^{-3}) (a), and together with pyronaridine at concentrations of 50 (b), 100 (c), 150 (d) and 200 (e) $\mu\text{mol dm}^{-3}$. *Inset* Effect of tryptophan concentration on the first-order rate for formation of the transient absorbance at 640 nm for the above solutions

Fig. 5 The transient absorption change in an N_2O -saturated solution at pH 7 containing APAP (4 mmol dm^{-3}) and pyronaridine (1 mmol dm^{-3}) recorded at 640 nm

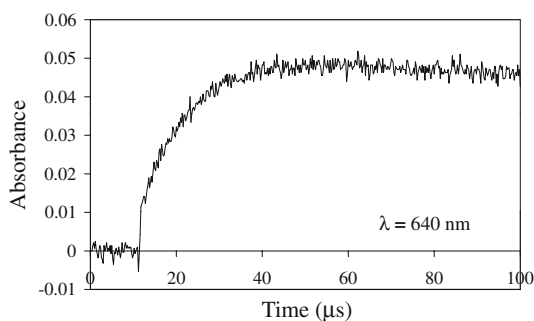
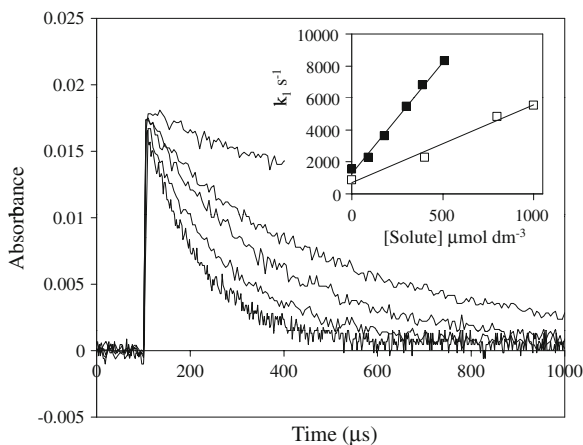


Fig. 6 Reduction of the pyronaridine radical recorded at 640 nm by pulse radiolysis of N_2O -saturated solutions of pyronaridine (1 mmol dm^{-3}) and NaN_3 (0.1 mol dm^{-3}) at pH 6.8 alone and with increasing concentrations of ascorbate (90, 180, 300 and 500 $\mu\text{mol dm}^{-3}$). *Inset* second-order plots for the reduction of pyronaridine radical absorption at 640 nm and pH 6.8 by ascorbate (filled square) and caffeic acid (open square)



These free radical interactions between species with known reduction potentials demonstrate that the one-electron reduction potential of the pyronaridine radical at neutral pH lies between that of APAP (707 mV) and caffeic acid (534 mV). It was not possible to undertake the usual experiments to determine transient equilibria with redox standards at high pH (>12) [20] due to the insolubility of pyronaridine under these conditions.

Decay of the pyronaridine radical

The radical described above formed from the one-electron oxidation of pyronaridine was unstable and decayed on a millisecond timescale. The decay of the difference spectrum at pH 6.7 is illustrated in Fig. 7. The radical peaks at 540 and 640 nm decay and are replaced by a much less intense residual absorbance peaking in the region of 550–600 nm. At all wavelengths, the decay could be fitted to a second-order process plus a residual product absorbance. The decay at 640 nm is shown in the inset of Fig. 7 and gives a second-order rate constant for decay ($2k_2$) of $(5.2 \pm 0.1) \times 10^8 \text{ dm}^3 \text{ mol}^{-1} \text{ s}^{-1}$. This value is based on an extinction coefficient of $4,700 \text{ dm}^3 \text{ mol}^{-1} \text{ cm}^{-1}$ at 640 nm, assuming quantitative oxidation of pyronaridine by azidyl radical. The observed second-order decay could be explained by either a radical termination (i.e. homo or hetero dimerisation) or a disproportionation reaction (Fig. 8). The latter appears to be more consistent with steric hindrance imposed by two methylene pyrrolidinyl groups occupying both *ortho*-phenolic positions and with the residual absorption found during pulse radiolysis. In this case, the product spectrum at 550–600 nm belongs to the iminoquinone that has been previously discussed in relation to the toxic side effects of this drug [6]. Preliminary PI-ESMS investigations of the products, from the radiolysis of a nitrous oxide saturated solution of pyronaridine containing sodium azide, have revealed the formation of the iminoquinone **3a** (Fig. 8). The mass spectra are shown in the Supplementary Material. Importantly, products arising from bimolecular termination reactions of pyronaridine radicals were not detected.

The structural details of pyronaridine and the one- and two-electron oxidised products were studied using density functional theory (DFT) methodology with the Gaussian03 program [29] to ascertain which route was thermodynamically favoured, since most investigators have assumed that disproportionation is the favoured decay mode (Fig. 8). Similar combined pulse radiolytic–DFT approaches have proved to be successful in explaining the decay of *ortho*-substituted transient semi-iminoquinones involved in pheomelanogenesis [30].

For the DFT study, the input model for pyronaridine (**1**) was built in two parts. First, the moiety based on the 7-chloro-2-methoxybenzo[*b*][1,5]naphthyridine heterocyclic system was attached via an NH substituent to a phenyl ring. There are only two variables, namely, the C1–C2–N1–C3 and C2–N1–C3–C4 torsion angles between the aromatic rings (see Fig. 9 for atom identification), and optimum values were obtained from previous calculations [31]. The second variable involves the orientations of the 4-amino-2,6-*bis*(pyrrolidin-1-ylmethyl)phenol fragment and we used experimental data from the CCDC [32]), in particular, DUTTUH, DUTVAP,

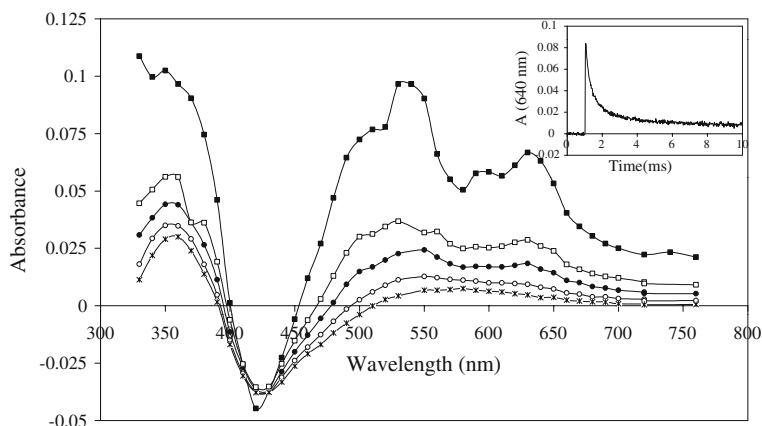


Fig. 7 Decay of the transient difference spectra on a millisecond timescale following pulse radiolysis of an N_2O -saturated solution of pyronaridine ($50 \mu\text{mol dm}^{-3}$) containing sodium azide (0.1 mol dm^{-3}) and phosphate buffer (20 mmol dm^{-3}) at pH 6.7. Spectra are shown at delays after pulses of $50 \mu\text{s}$ (filled square), $200 \mu\text{s}$ (open square), $500 \mu\text{s}$ (filled diamond), 1.5 ms (open circle) and 8 ms (asterisks). Inset Decay of the transient absorption at 640 nm

SOPBEE and VIMYEV, which had very similar conformations. The resulting complete structural model was then fully optimised; subsequently, starting models for **2a**, **2b** and **3a** were built by removing the appropriate hydrogen atom(s) from the optimised one and then fully optimised using the UB3LYP/6-31+G* methodology.

The enthalpies of the reactions $1-\text{H}^\bullet \rightarrow 2\text{a}$ and $1-\text{H}^\bullet \rightarrow 2\text{b}$ were then studied. All entities were geometry-optimised and the enthalpies of the reactions were calculated as 87.1 and $87.6 \text{ kcal mol}^{-1}$, respectively. Therefore, there is little significant difference between the energies of the phenoxyl and aminyl radicals. These values compare favourably with the free energy ($76.7 \text{ kcal mol}^{-1}$) for that found in the related molecule 4,6-di-tert-butyl-2-tert-butylimino-semiquinone in which the phenoxyl group is also sterically hindered [33].

In contrast, the enthalpy of the reaction $1-2\text{H}^\bullet \rightarrow 3\text{a}$ was calculated as $154.97 \text{ kcal mol}^{-1}$. This can be compared favourably with the enthalpies for the formation of $2\text{a} + 2\text{b}$, or, indeed, $2 * 2\text{a}$ or $2 * 2\text{b}$, which would have a combined enthalpy of ca $175 \text{ kcal mol}^{-1}$. Thus, the disproportionation reaction of radicals **2a** and **2b** to form **3a** is favoured by ca 20 kcal mol^{-1} , a result concordant with the ESMS evidence.

The structures of **1**, **2a**, **2b** and **3a** are shown in Fig. 9, with their important dimensions compared in Table 2.

It will be noted that there is, as expected, a significant change in geometry when the hydrogen on N1 is removed in **3a**. The main change is a decrease in the N1–C3 bond length by 0.136 \AA , which is accompanied by a change in conformation as the C2–N1–C3–C4 torsion angle changes from 139.4° to -173.6° , so that the arrangement around the C3–N1 double bond is approximately planar. This increase in conjugation will cause a corresponding shift in the product absorption maximum, as observed experimentally for the iminoquinone product in Fig. 7. By contrast, the

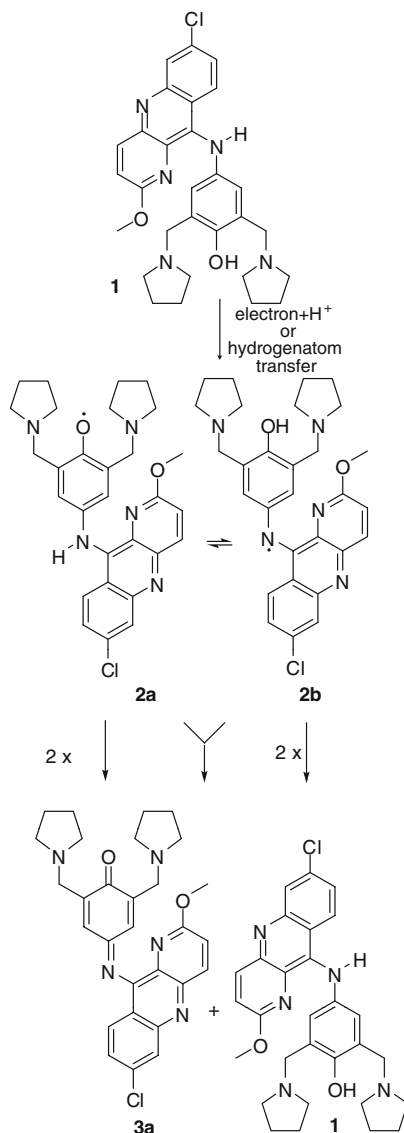


Fig. 8 Disproportionation of pyronaridine radicals. **1**: pyronaridine; **2a**: phenoxyl radical; **2b**: aminyl radical; **3a**: pyronaridine iminoquinone: 4-(7-chloro-2-methoxybenzo[*b*][1,5]naphthyridin-10-ylimino)-2,6-bis(pyrrolidin-1-ylmethyl)cyclohexa-2,5-dienone)

C1–C2–N1–C3 torsion angle changes from 145.3° in **1** to 62.5° in **3a**, twisting further away from planarity and concomitant with a slight increase in the C2–N1 bond length, which has less double-bond character, increasing slightly from 1.375 to 1.385 Å. The structures of the radicals **2a** and **2b** show some variations. In **2a**, the C–O7 bond length is 1.257 Å, close to that for a double bond; the C–C bonds in the six-membered ring starting adjacent to the carbonyl are 1.469, 1.376, 1.418, 1.421,

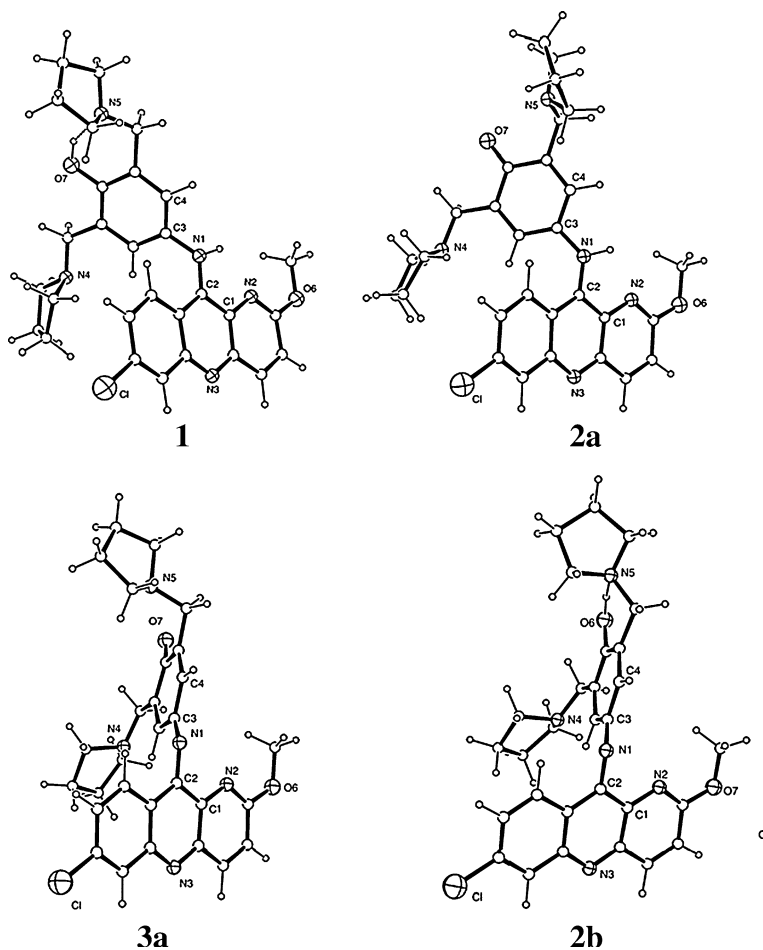


Fig. 9 Structures of pyronaridine **1**, the two radicals **2a** and **2b**, and the iminoquinone **3a**

Table 2 Dimensions in **1**, **2a**, **2b** and **3a**: distances, Å; torsion angles, °

	1	2a	2b	3a
C2–N1	1.375	1.388	1.401	1.385
N1–C3	1.432	1.393	1.343	1.296
C1–C2–N1–C3	145.3	135.5	63.4	62.5
C2–N1–C3–C4	139.4	172.2	–170.9	–173.6
O7...N5	2.718	3.361	2.686	3.338

1.373 and 1.466 Å, showing that the ring loses some of its aromatic character but not all. Thus, the comparable distances in the iminoquinone **3a** are 1.492, 1.349, 1.464, 1.466, 1.349 and 1.493 Å. The N1–C3 in the **2a** bond has slightly more

double-bond character than in **1** and the C2–N1–C3–C4 torsion angle increases to 172.2°. By contrast, the torsion angles in **2b** are almost exactly the same as in **3a**. The N1–C3 bond length at 1.343 Å retains some double-bond character, but is still significantly longer than the 1.296 Å found in **3a**.

There is an additional change in that in **1**, there is an intramolecular hydrogen bond between O7–H and N5 with an O7...N5 distance of 2.718 Å. This is maintained in **2b** with a distance of 2.686 Å, but with the removal of the hydrogen atom on O7, as in **2a** or **3a**, this distance increases to 3.361 and 3.338 Å, respectively. These results are consistent with the conclusions drawn in Sect. 1 that the aminophenol moiety is the reaction site with oxidising free radicals. Radicals such as **2a** and/or **2b** could arise through the interaction of oxidisable groups with free haeme(II) released during the parasite-mediated catabolism of haemoglobin [34] and could contribute, in part, to the antimalarial action of compounds containing the *para*-amino phenol moiety [3].

Conclusions

Pyronaridine is readily oxidised to the radical species with a one-electron reduction potential at pH 7 for the radical species between ca. 530 and 700 mV, as defined by observed reactions with caffeic acid and the acetaminophen semi-iminoquinone radical, respectively. The result shows that pyronaridine is more readily oxidised than acetaminophen and accounts for the ease with which the drug is metabolised to potentially toxic intermediates [6, 35]. The radical decays by a second-order process, which is suggested on the basis of spectral evidence, mass spectrometry and calculation to be a disproportionation resulting in the formation of the iminoquinone that may be responsible for reaction with thiols and protein conjugation in vivo. In a recent Phase II trial in which potentially hypersensitive paediatric patients were excluded, each patient encountered at least one life-threatening adverse event which could be associated with using a combination of pyronaridine-artesunate [36]. These investigators prudently emphasise that “the tolerability of pyronaridine-artesunate will be fully established only by larger randomized controlled trials and postmarketing surveys.”

Acknowledgements We thank Professor David Warhurst (London School of Tropical Medicine and Hygiene) for the kind gift of the pyronaridine sample and to Said Alizadeh-Shekalgourabi for synthesising the SA48. We also thank STFC and Daresbury Laboratory for providing access to the linear accelerator at the Synchrotron Radiation Source for pulse radiolysis studies and Dr. Ruth Edge and Ms. Ana G. Crisostomo for their assistance with the experiments. Ms. Nicola M. Dempster provided expert technical assistance in performing all of the positive-ion electrospray mass spectrometry experiments.

References

1. M. Schlitzer, Antimalarial drugs—what is in use and what is in the pipeline. Arch. Pharm. Chem. Life Sci. **341**, 149–163 (2008)

2. W. Peters, B.L. Robinson, The chemotheropy of rodent malaria. 47. Studies on pyronaridine and other Mannich base antimalarials. *Ann. Trop. Med. Parasitol.* **86**, 455–465 (1992)
3. M.J. Dascombe, M.G.B. Drew, P.G. Evans, F.M.D. Ismail, Rational design strategies for the development of synthetic quinoline and acridine based antimalarials. *Front. Drug Design Disc.* **3**, 559–609 (2007)
4. K.A. Neftel, W. Woodtly, M. Schmid, P.G. Frick, J. Fehr, Amodiaquine induced agranulocytosis and liver damage. *Br. Med. J.* **292**, 721–723 (1986)
5. J.L. Maggs, M.D. Tingle, N.R. Kitteringham, B.K. Park, Drug–protein conjugates—XIV. Mechanisms of formation of protein-aryllating intermediates from amodiaquine, a myelotoxin and hepatotoxin in man. *Biochem. Pharmacol.* **37**, 303–311 (1988)
6. D.J. Naisbitt, D.P. Williams, P.M. O'Neill, J.L. Maggs, D.J. Willock, M. Pirmohamed, B.K. Park, Metabolism-dependent neutrophil cytotoxicity of amodiaquine: a comparison with pyronaridine and related antimalarial drugs. *Chem. Res. Toxicol.* **11**, 1586–1595 (1998)
7. P.M. O'Neill, P.G. Bray, S.R. Hawley, S.A. Ward, B.K. Park, 4-aminoquinolines—past, present, and future: a chemical perspective. *Pharmacol. Ther.* **77**, 29–58 (1998)
8. P.M. O'Neill, A. Mukhtar, P.A. Stocks, L.E. Randle, S. Hindley, S.A. Ward, R.C. Storr, J.F. Bickley, I.A. O'Neil, J.L. Maggs, R.H. Hughes, P.A. Winstanley, P.G. Bray, B.K. Park, Isoquine and related amodiaquine analogues: a new generation of improved 4-aminoquinoline antimalarials. *J. Med. Chem.* **46**, 4933–4945 (2003)
9. U. Jurva, A. Holmén, G. Grönberg, C. Masimiremba, L. Weidolf, Electrochemical generation of electrophilic drug metabolites: characterization of amodiaquine quinoneimine and cysteinyl conjugates by MS, IR, and NMR. *Chem. Res. Toxicol.* **21**, 928–935 (2008)
10. S.D. Nelson, Mechanisms of the formation and disposition of reactive metabolites that can cause acute liver injury. *Drug Metab. Rev.* **27**, 147–177 (1995)
11. O.A. Adegoke, C.P. Babalola, O.S. Oshitade, A.A. Famuyiwa, Determination of the physicochemical properties of pyronaridine—a new antimalarial drug. *Pak. J. Pharm. Sci.* **19**, 1–16 (2006)
12. S.A. Gamage, N. Tepsiri, P. Wilairat, S.J. Wojcik, D.P. Figgitt, R.K. Ralph, W.A. Denny, Synthesis and in vitro evaluation of 9-anilino-3,6-diaminoacridines active against a multidrug-resistant strain of the malaria parasite *Plasmodium falciparum*. *J. Med. Chem.* **37**, 1486–1494 (1994)
13. P. Chavalitshewinkoon, P. Wilairat, S. Gamage, W. Denny, D. Figgitt, R. Ralph, Structure–activity relationships and modes of action of 9-anilinoacridines against chloroquine-resistant *Plasmodium falciparum* in vitro. *Antimicrob. Agents Chemother.* **37**, 403–406 (1993)
14. G. Padmanaban, P.N. Rangarajan, Heme metabolism of *Plasmodium* is a major antimalarial target. *Biochem. Biophys. Res. Commun.* **268**, 665–668 (2000)
15. N.H. Hunt, R. Stocker, Heme moves to center stage in cerebral malaria. *Nat. Med.* **13**, 667–669 (2007)
16. D. Jani, R. Nagarkatti, W. Beatty, R. Angel, C. Slebodnick, J. Andersen, S. Kumar, D. Rathore, HDP—a novel heme detoxification protein from the malaria parasite. *PLoS Pathog.* **4**, e1000053 (2008)
17. S. Pagola, P.W. Stephens, D.S. Bohle, A.D. Kosar, S.K. Madsen, The structure of malaria pigment beta-haematin. *Nature* **404**, 307–310 (2000)
18. M.J. Dascombe, M.G.B. Drew, H. Morris, P. Wilairat, S. Auparakkitanon, W.A. Moule, S. Alizadeh-Shekalgourabi, P.G. Evans, M. Lloyd, A.M. Dyas, P. Carr, F.M.D. Ismail, Mapping antimalarial pharmacophores as a useful tool for the rapid discovery of drugs effective in vivo: design, construction, characterization, and pharmacology of metaquine. *J. Med. Chem.* **48**, 5423–5436 (2005)
19. S. Auparakkitanon, S. Chapoomram, K. Kuaha, T. Chirachariyavej, P. Wilairat, Targeting of hematin by the antimalarial pyronaridine. *Antimicrob. Agents Chemother.* **50**, 2197–2200 (2006)
20. S. Steenken, P. Neta, One-electron redox potentials of phenols. Hydroxy- and aminophenols and related compounds of biological interest. *J. Phys. Chem.* **86**, 3661–3667 (1982)
21. P. Neta, Radiation chemistry of quinoid compounds, in *The chemistry of quinoid compounds*, vol. II, ed. by S. Patai, Z. Rappoport (Wiley, Chichester, 1988), pp. 879–898
22. R.H. Bisby, N. Tabassum, Properties of the radicals formed by one-electron oxidation of acetaminophen—a pulse radiolysis study. *Biochem. Pharmacol.* **37**, 2731–2738 (1988)
23. R.H. Bisby, Reactions of a free radical intermediate in the oxidation of amodiaquine. *Biochem. Pharmacol.* **39**, 2051–2055 (1990)
24. D.M. Stout, W.L. Matier, C. Barcelon-Yang, R.D. Reynolds, B.S. Brown, Synthesis and antiarrhythmic and parasympholytic properties of substituted phenols. I. Heteroarylamine derivatives. *J. Med. Chem.* **26**, 808–813 (1983)

25. D.J. Holder, D. Allan, E.J. Land, S. Navaratnam, Establishment of pulse radiolysis facility on the SRS linac at Daresbury Laboratory, in *Proceedings of the 8th European Particle Accelerator Conference*, Paris, France, pp. 2804–2806, European Physical Society (2002)
26. P. Wardman, Reduction potentials of one-electron couples involving free radicals in aqueous solution. *J. Phys. Chem. Ref. Data* **18**, 1637–1755 (1989)
27. A. Harriman, Further comments on the redox potentials of tryptophan and tyrosine. *J. Phys. Chem.* **91**, 6102–6104 (1987)
28. S. Foley, S. Navaratnam, D.J. McGarvey, E.J. Land, T.G. Truscott, C.A. Rice-Evans, Singlet oxygen quenching and the redox properties of hydroxycinnamic acids. *Free Radic. Biol. Med.* **26**, 1202–1208 (1999)
29. M.J. Frisch, G.W. Trucks, H.B. Schlegel, G.E. Scuseria, M.A. Robb, J.R. Cheeseman, J.A. Montgomery Jr., T. Vreven, K.N. Kudin, J.C. Burant, J.M. Millam, S.S. Iyengar, J. Tomasi, V. Barone, B. Mennucci, M. Cossi, G. Scalmani, N. Rega, G.A. Petersson, H. Nakatsuji, M. Hada, M. Ehara, K. Toyota, R. Fukuda, J. Hasegawa, M. Ishida, T. Nakajima, Y. Honda, O. Kitao, H. Nakai, M. Klene, X. Li, J.E. Knox, H.P. Hratchian, J.B. Cross, V. Bakken, C. Adamo, J. Jaramillo, R. Gomperts, R.E. Stratmann, O. Yazyev, A.J. Austin, R. Cammi, C. Pomelli, J.W. Ochterski, P.Y. Ayala, K. Morokuma, G.A. Voth, P. Salvador, J.J. Dannenberg, V.G. Zakrzewski, S. Dapprich, A.D. Daniels, M.C. Strain, O. Farkas, D.K. Malick, A.D. Rabuck, K. Raghavachari, J.B. Foresman, J.V. Ortiz, Q. Cui, A.G. Baboul, S. Clifford, J. Cioslowski, B.B. Stefanov, G. Liu, A. Liashenko, P. Piskorz, I. Komaromi, R.L. Martin, D.J. Fox, T. Keith, M.A. Al-Laham, C.Y. Peng, A. Nanayakkara, M. Challacombe, P.M.W. Gill, B. Johnson, W. Chen, M.W. Wong, C. Gonzalez, J.A. Pople, *Gaussian 03, Revision C.02* (Gaussian, Inc., Wallingford, CT, 2004)
30. A. Pezzella, O. Crescenzi, A. Natangelo, L. Panzella, A. Napolitano, S. Navaratnam, R. Edge, E.J. Land, V. Barone, M. d'Ischia, Chemical, pulse radiolysis and density functional studies of a new, labile 5,6-indolequinone and its semiquinone. *J. Org. Chem.* **72**, 1595–1603 (2007)
31. V. Male, Computational studies of anti-malarials, M.Sc. Thesis, Department of Chemistry, University of Reading (2003)
32. Cambridge Crystallographic Data Centre, August 2008 update. Home page at: <http://www.ccdc.cam.ac.uk>
33. S.M. Carter, A. Sia, M.J. Shaw, A.F. Heyduk, Isolation and characterization of a neutral imino-semiquinone radical. *J. Am. Chem. Soc.* **130**, 5838–5839 (2008)
34. D. Monti, B. Vodopivec, N. Basilico, P. Olliaro, D. Taramelli, A novel endogenous antimalarial: Fe(II)-Protoporphyrin IX α (heme) inhibits hemozoin polymerization to β -hemozoin (malaria pigment) and kills malaria parasites. *Biochemistry* **38**, 8858–8863 (1999)
35. J. Lee, J. Son, S.-J. Chung, E.-S. Lee, D.-H. Kim, In vitro and in vivo metabolism of pyronaridine characterized by low-energy collision-induced dissociation mass spectrometry with electrospray ionization. *J. Mass Spectrom.* **39**, 1036–1043 (2004)
36. M. Ramharter, F. Kurth, A.C. Schreier, J. Nemeth, I. von Glasenapp, S. B elard, M. Schlie, J. Kammer, P.K. Koumba, B. Cisse, B. Mordm uller, B. Lell, S. Issifou, C. Oeuvray, L. Fleckenstein, P.G. Kremsner, Fixed-dose pyronaridine-artesunate combination for treatment of uncomplicated falciparum malaria in pediatric patients in Gabon. *J. Infect. Dis.* **198**, 911–919 (2008)